Interface states in carbon nanotube junctions: Rolling up graphene

H. Santos,[1] A. Ayuela,[2] W. Jaskólski,[3] M. Pelc,[3] and L. Chico[1]
[1]*Instituto de Ciencia de Materiales de Madrid, Consejo Superior de Investigaciones Científicas, Cantoblanco, 28049 Madrid, Spain*
[2]*Departamento de Física de Materiales (Facultad de Químicas), Centro de Física de Materiales CFM-CPM CSIC-UPV/EHU and Donostia International Physics Center (DIPC), 20080 San Sebastián/Donostia, Spain*
[3]*Instytut Fizyki UMK, Grudziadzka 5, 87-100 Toruń, Poland*
(Received 14 July 2009; published 31 July 2009)

We study the origin of interface states in carbon nanotube intramolecular junctions between achiral tubes. By applying the Born-von Karman boundary condition to an interface between armchair- and zigzag-terminated graphene layers, we are able to explain their number and energies. We show that these interface states, costumarily attributed to the presence of topological defects, are actually related to zigzag-edge states, as those of graphene zigzag nanoribbons. Spatial localization of interface states is seen to vary greatly and may extend appreciably into either side of the junction. Our results give an alternative explanation to the unusual decay length measured for interface states of semiconductor nanotube junctions and could be further tested by local probe spectroscopies.

DOI: 10.1103/PhysRevB.80.035436 PACS number(s): 73.22.−f, 73.20.−r

I. INTRODUCTION

Carbon nanotubes (CNT) are currently regarded as one of the most promising materials to develop future nanoelectronics, with an impressive combination of robustness and ideal electronic properties. At present, it is well established that further progress toward real applications depends on the ability to form junctions between different nanotubes.[1] Recently, the controlled synthesis of several carbon nanotube intramolecular junctions has been reported, either by current injection between nanotubes[2] or by temperature changes during growth.[3] These intramolecular junctions, which often present interface states (IS), are typically made of topological defects arising from the connection between tubes of different chirality. In fact, the interplay between defects and charge transport is a central motivation of CNT research in the fabrication of electronic devices such as diodes[4] or transistors.[5]

For example, although interface states are commonly regarded as a drawback in device performance, they may actually provide a means of achieving diode behavior at the nanoscale, as proposed in Ref. 6. In any case, transport spectroscopy experiments have shown that interface states play an important role in the behavior of CNT junctions.[7–9] On the one hand, Ishigami *et al.*[8] studied interface states in metal/metal CNT junctions with scanning tunneling microscopy, showing that interface states extended approximately 2 nm from the junction. On the other hand, Kim *et al.*[9] found longer decay lengths for semiconductor nanotube junctions, with different values at each side of the interface. Therefore, understanding the physics of CNT intramolecular junctions, for which interface states close to the Fermi energy may dominate transport properties, has been a subject of growing activity in the last few years.[10–14] A fundamental question regarding interface states is to study their systematics and their origin.

In this work, we explain the appearance of interface states in carbon nanotube junctions made of achiral tubes. To achieve this, we have performed a systematic study of these states for a sufficiently large set of junctions, identifying the regularities in the energies and number of such states. Then, we have studied a related system, an armchair-terminated semi-infinite graphene joined to a zigzag-terminated one. Such system presents an interface band, from which the nanotube interface states can be derived. Analogously to the obtention of a carbon nanotube by rolling a graphene strip, an achiral carbon nanotube junction can be obtained rolling up a portion of the zigzag/armchair graphene junction. Thus, by applying Born-von Karman boundary condition to the interface band found for the graphene junction, we obtain the number and energies of the carbon nanotube interface states. The study of the zigzag-terminated graphene allows us to identify this interface band as a zigzag-edge state in graphene, thus unraveling the origin of interface states in carbon nanotube achiral junctions. We have confirmed our results by first-principles calculations for the smallest junctions, showing the adequateness of our approach.

The rest of the paper is organized as follows. In Sec. II we describe the systems studied and briefly outline the calculation methods employed. Section III is devoted to the results and discussion and in Sec. IV we summarize our main conclusions.

II. MODEL AND METHOD

The main purpose of this paper is to describe interface states and elucidate their origin by studying junctions of varying diameter. Specifically, we address the energy spectra of achiral nanotube intramolecular junctions. Zigzag/armchair junctions are made by joining a $(2n,0)$ and an (n,n) tube; this is achieved with a ring of n pentagon-heptagon defect pairs. In Fig. 1 we show a particular example of this kind of junctions, namely, the (10,0)/(5,5) case, with a ring of 5 pentagon-heptagon (5/7) defects forming the union between the tubes. We have performed the systematic study of carbon nanotube junctions within the π-electron tight-binding approximation.[15] As the junctions lack translational periodicity, we employ a Green's-function matching technique to calculate the local density of states in carbon

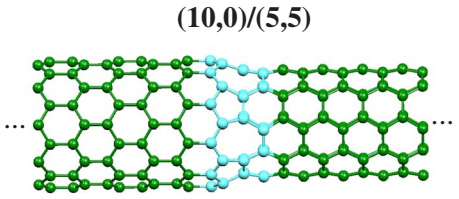

FIG. 1. (Color online) Geometry of a (10,0)/(5,5) junction, with the atoms comprising the ring of pentagon-heptagon defects in a different color.

nanotube and graphene junctions; details are given in Ref. 12. We have recently shown that for multiple junctions, like $N(12,0)/M(6,6)$ superlattices (SLs), this approximation yields the electronic structure around the Fermi energy (E_F) in good agreement with the results from first-principles calculations.[16]

Notwithstanding, to assess the validity of the tight-binding results presented here, we have checked that the number of interface states given with this simpler method agrees with that obtained with an *ab initio* approach for the smaller system sizes, up to $n=7$. The first-principles calculations were carried out using the generalized gradient approximation within density-functional theory[17] employing the SIESTA *ab initio* method.[18] Core electrons were described using the Troulliers-Martin norm-conserving pseudopotentials while valence electrons are described with double ξ singly polarized basis set. Real-space integration is performed on a regular grid corresponding to a plane-wave cutoff of 150 eV. In order to use the supercell approach, we have calculated the superlattices corresponding to the junctions of interest, thus periodically repeating the interfaces. The calculated cases are 8(6,0)/8(3,3), 4(8,0)/4(4,4), 4(12,0)/4(6,6), and 4(14,0)/4(7,7), where the prefactor N in $N(n,m)$ indicates the number of unit cells employed for the superlattices. We have taken 8 points in the Brillouin zone (BZ), which is twice the number required for the meV accuracy of previous calculations.[16] Perpendicular to their axis, the distances in the supercell are larger than 45 Å so we can neglect their interaction. The atomic coordinates have been relaxed until the forces are below 0.04 eV/Å.

III. RESULTS AND DISCUSSION

A. Carbon nanotube junctions

In Fig. 2 we show the local density of states around E_F evaluated at the junction, for all $(2n,0)/(n,n)$ systems from $n=4$ to $n=15$. The first interface state appears for $n=4$; smaller junctions, such as the (6,0)/(3,3) case (not shown), have no localized states even though they have a full ring of 5/7 topological defects. Clearly, IS obey a multiple-of-three rule: when $n=3q+1$, with $q=1,2,\ldots$ a new interface state appears, q being the number of such states. Each interface state can be labeled by an integer number m, characterizing the behavior of the wave function Ψ_{IS} under rotations C_n of an angle $\phi=2\pi/n$. As the junction is invariant under C_n, it follows that $C_n\Psi_{\mathrm{IS}}=e^{im\phi}\Psi_{\mathrm{IS}}$. In Fig. 2 interface states of equal m are joined with a dashed line. The label m can be

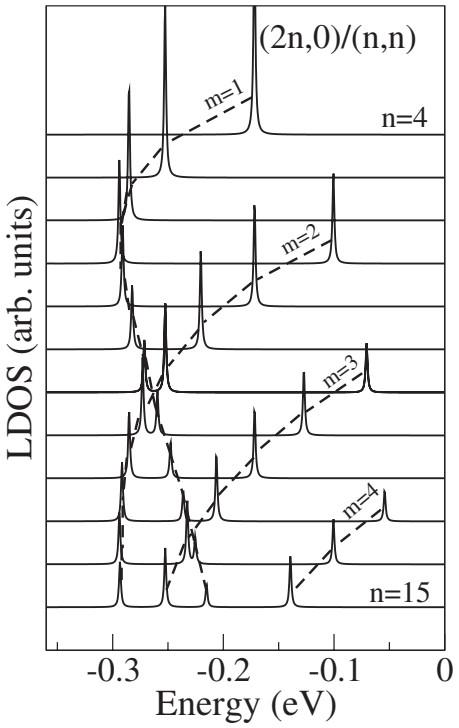

FIG. 2. Local density of states below the Fermi level vs n for a series of $(2n,0)/(n,n)$ junctions. Peaks correspond to interface states. The curves are arranged from top to bottom in order of increasing n, with the smallest and largest values indicated therein. Dashed lines are guides to the eyes.

viewed as a "discrete angular momentum" quantum number.[12] The behavior of interface states is reminiscent of localized states in a quantum-well system with increasing number of layers.[19] However, in contradistinction to quantum-well states, these interface peaks cross with increasing system size. Another key feature is that their energies are limited to a narrow interval below E_F, specifically, between −0.3 and 0 eV, as can be seen in the figure.

Additionally, notice that some interface states at junctions with different n have exactly the same energies. Such are, for example, the (8,0)/(4,4), the (16,0)/(8,8), and the (24,0)/(12,12) junctions, which have one interface state at −0.172 eV, the (12,0)/(6,6) and the (24,0)/(12,12) junctions, with one IS at −0.285 eV. The coincidence in energies for some interface states and the regularity in their appearance point toward their folding origin.

B. Armchair/zigzag graphene junction

In order to understand the features of the interface states described above, we have turned to a system closely related to this series of nanotube junctions; a semi-infinite zigzag graphene joined to an armchair-terminated one, yielding an infinite line of pentagon-heptagon topological defects as interface between the two graphene edges. The geometry of this graphene junction is shown in Fig. 3. In the same way that a perfect nanotube is made by rolling up a graphene sheet, a carbon nanotube junction like those described above

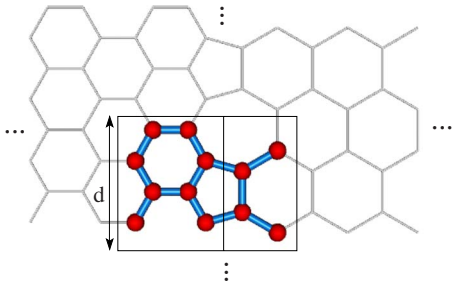

FIG. 3. (Color online) Geometry of the zigzag/armchair graphene junction. The two rectangles show the unit cells employed in the Green's-function matching calculation of interface bands.

can be obtained by rolling up a strip of these matched semi-infinite graphenes.

The band structure of the graphene armchair/zigzag interface is shown in the left panel of Fig. 4, along with the projected bulk bands at this interface; the right panel depicts the edge band of zigzag-terminated graphene with the corresponding projected graphene bulk band structure at this surface. The interface band shown in the left panel spans from Γ to 2/3 of the positive part of the Brillouin zone. Note that just at the edge points there are no interface states because they belong to the bulk of the armchair- and the zigzag-terminated graphene, respectively. The graphene interface band spans from −0.3 eV to 0 eV, comprising the energy range of all the nanotube interface states. Rolling up the graphene junction

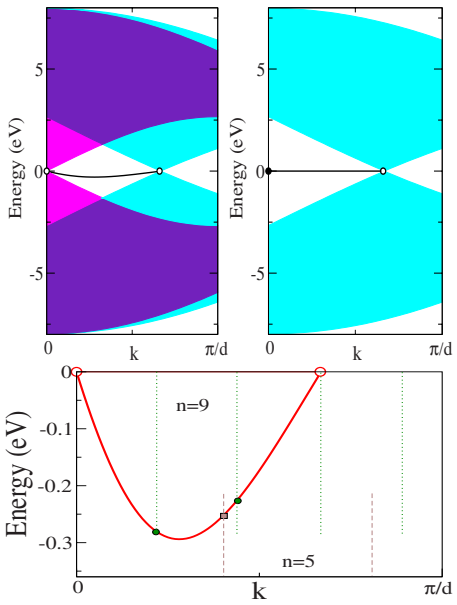

FIG. 4. (Color online) Left panel: Interface band of the zigzag/armchair graphene junction, with the corresponding projected graphene bulk bands at this interface. Right panel: edge band of the zigzag-terminated graphene with the graphene band structure projected at this surface. Bottom panel: zoom of the interface band, with quantization lines showing the interface energies for the $n=5$ (dashed) and the $n=9$ junctions (dotted). Symbols mark the corresponding interface state energies. Open circles at the interface band ends stress that these energies do not belong to the band but, rather, to the bulk continua.

amounts to imposing Born-von Karman boundary condition to the graphene interface band. This determines the quantization rule

$$k = \frac{2\pi m}{nd}, \quad m = 0, \ldots, n-1, \tag{1}$$

where d is the length of the repeat unit along the interface and n is the number of repetitions to give a $(2n,0)/(n,n)$ junction. The index m is the same "discrete angular momentum" label formerly introduced. The allowed k values give the nanotube interface states shown in Fig. 2, as demonstrated graphically for two examples, namely, $n=5$ and $n=9$, in the bottom panel of Fig. 4. The energies obtained by this rule exactly match those obtained in the nanotube junction calculations, collected in Fig. 2. The multiple-of-three periodicity is thus understood, due to the length of the BZ portion in which the interface graphene band exists, i.e., 2/3 of its irreducible part. Furthermore, within the model employed, it is now clear why for $n<4$ there are no interface states in the $(2n,0)/(n,n)$ junctions; in these cases, quantization lines touch the edges of the graphene interface band and these end points do not actually belong to it because they are in the zigzag and armchair graphene bulk continua. Finally, the appearance of interface states with exactly the same energies is simply explained by the quantization rule given in Eq. (1).

C. Armchair and zigzag graphene-free edges

To clarify the origin of the interface band found for the zigzag/armchair graphene junction, we have analyzed the corresponding graphene-free "surfaces," the armchair-terminated and the zigzag-terminated semi-infinite graphenes.[20] No surface bands appear in the gap of the armchair-terminated graphene whereas for the zigzag-terminated one, shown in the right panel of Fig. 4, a flat band at 0 eV spans from Γ to 2/3 of the irreducible part of the BZ. For the purposes of direct comparison, we use the same unit cell as for the interface calculation, which is doubled with respect to the one usually employed for zigzag geometry. Note that the $k=0$ state belongs to the surface band, given that it is in the bulk gap; this explains why all semi-infinite $(2n,0)$ zigzag nanotubes have a "surface" edge state at 0 eV. Joining the zigzag-edge graphene to the armchair one breaks the electron-hole symmetry due to the mixing of the two graphene sublattices, combing the surface band and moving it to negative energies, as depicted in the left panel of Fig. 4. Thus, the armchair-edge graphene acts as an external potential for the states of the zigzag-terminated graphene, bending down the interface band. The zigzag-edge nature of the interface band shown in Fig. 4 is therefore demonstrated, as well as that of interface states in zigzag/armchair junctions of tubes, which we have shown here to originate from edge states, as those found in graphene nanoribbons. This finding has implications for the analysis of other defects such as vacancies and even substitutional atoms in nanotubes or graphene, which have been shown to yield an effective edge in the hexagonal carbon lattice.[21]

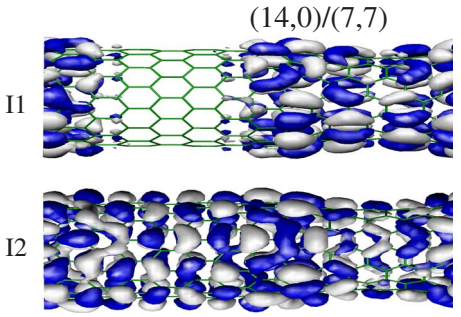

FIG. 5. (Color online) Two examples of wave functions of interface states belonging to the 4(14,0)/4(7,7) superlattice calculated *ab initio*.

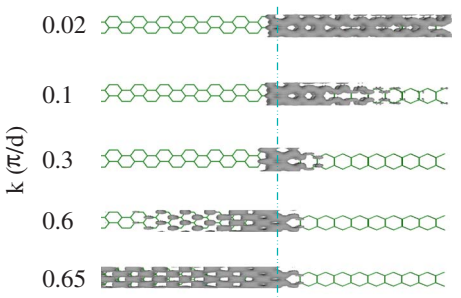

FIG. 6. (Color online) Electron density of several states belonging to the interface band of the graphene armchair/zigzag junction, calculated with a π-orbital tight-binding model.

D. First-principles calculations of nanotube superlattices

In order to test the robustness of our tight-binding results, we have performed *ab initio* calculations of $4(2n,0)/4(n,n)$ SLs using the method and parameters described in Sec. II. Introducing another junction and imposing periodic boundary conditions induces significant changes in the electronic structure but by comparison to tight-binding results and checking the wave-function symmetry and spatial distribution, we have successfully identified interface states.[22] Specifically, we have checked that there are no interface states in the (6,0)/(3,3) system whereas one IS per junction appears in the (8,0)/(4,4) and the (12,0)/(6,6) cases, and two states per junction appear in the (14,0)/(7,7) system. For the time being, further studies for lattices with a larger number of defects are beyond our computational capabilities. Hitherto, *ab initio* calculations and tight-binding results fully agree as to the number of interface states in these achiral junctions.

We have chosen a pair of interface states belonging to the largest system calculated by *ab initio* techniques, namely, the 4(14,0)/4(7,7) SL, to show their spatial distribution. Their wave functions are shown in Fig. 5. The lowest-lying interface state, labeled I1, is mainly localized at the interface, spreading toward the armchair side. This behavior was also observed in the interface states of (12,0)/(6,6) SLs and (10,0)/(5,5) junctions.[6,22] But, surprisingly, the second interface state (labeled I2) spreads appreciably from the interface into the zigzag part.

E. Spatial localization of interface states

To make sense of these disparate behaviors, we turn back to the graphene junction. Figure 6 depicts the electron density of several graphene interface states with different k values; states are labeled with the corresponding k value in π/d units. When moving from Γ to the interface band edge at 2/3 of the BZ, the wave-function localization changes from the armchair to the zigzag side; for k at the band minimum the wave function is mainly localized at the junction. This explains why the interface state of the (12,0)/(6,6) junction, which stems from the graphene $k=1/3$ state, is rather localized at the interface. Thus, the junctions with sufficiently large diameter will have different interface states spreading at opposite sides of the interface but pinned at the carbon ring made of 5/7 topological defects.

F. Relation to experiments and perspectives

Our results provide an alternative explanation to the unequal decay lengths found in semiconductor nanotube junctions, as well as to their large value compared to metallic systems.[8,9] The coexistence in the same nanotube of interface states with dissimilar spatial localization could be demonstrated by scanning tunneling microscopy and spectroscopy, as in Refs. 7–9. The fact that CNT junctions may have several interface states with different spatial localizations opens a way for new device design based on their characteristics. Choosing a CNT of appropriate diameter, states with quite different spatial localization can be accessed by applying different voltages, allowing for switch operation. Furthermore, due to interface charge localization and redistribution CNT junctions can act as chemically active sites. Actually, doping the interfaces may induce a structural reconstruction and alter their symmetry, thus dramatically changing the electronic properties because of the Fermi-level proximity to the IS.

Finally, although we have focused on junctions between achiral tubes and found that their interface states have zigzag-edge origin, we would like to note that differences in chirality of joined tubes plays a role. For example, a zigzag (8,0)/(7,1) junction has no interface states while the (8,0)/(5,3) junction has two.[10] We have chosen to study junctions between tubes with maximum difference in chiral angles. The nontrivial role of chirality deserves further exploration but in any case, our present results suggest that IS in chiral systems will also have edge origin.

IV. CONCLUSIONS

In summary, we have explored the nature of interface states in carbon nanotube junctions, focusing on achiral systems. We have shown that these states, usually attributed to the pentagon-heptagon topological defects, are actually due to the zigzag-edge-terminated nanotube. Topological defects break the electron symmetry and consequently make these states energy dependent. Furthermore, we have related these interface states of nanotube junctions to the interface band appearing in a graphene zigzag/armchair junction. By applying the Born-von Karman boundary condition to the

graphene interface band, we have derived the energies and number of the nanotube interface states, obtaining complete quantitative agreement with the CNT junction calculations. Unequal decay lengths found in the spatial localizations of interface states can be understood in the light of our findings. Our results give a surprising vision on the nature of CNT interface states and have implications in other systems such as graphene vacancies or substitutional impurities.

ACKNOWLEDGMENTS

L.C. acknowledges helpful discussions with J. I. Cerdá. This work has been partially supported by the Spanish DGES under Grants No. MAT2006-06242 and No. FIS2007-66711-C02-C01 and Spanish CSIC under Grant No. PI 200860I048. W.J. and M.P. acknowledge financial support from Polish LFPPI.

[1] D. Wei and Y. Liu, Adv. Mater. **20**, 2815 (2008).
[2] C. Jin, K. Suenaga, and S. Iijima, Nat. Nanotechnol. **3**, 17 (2008).
[3] Y. Yao, Q. Li, J. Zhang, R. Liu, L. Jiao, Y. T. Zhu, and Z. Liu, Nature Mater. **6**, 283 (2007).
[4] P. G. Collins, A. Zettl, H. Bando, A. Thess, and R. E. Smalley, Science **278**, 100 (1997); J. U. Lee, P. P. Gipp, and G. M. Heller, Appl. Phys. Lett. **85**, 145 (2004).
[5] S. J. Tans, A. R. M. Verschueren, and C. Dekker, Nature (London) **393**, 49 (1998); Z. Chen, J. Appenzeller, Y.-M. Lin, J. Sippel-Oakley, A. G. Rinzler, J. Tang, S. J. Wind, P. M. Solomon, and Ph. Avouris, Science **311**, 1735 (2006).
[6] A. Rochefort and Ph. Avouris, Nano Lett. **2**, 253 (2002).
[7] H. Kim, J. Lee, S.-J. Kahng, Y.-W. Son, S. B. Lee, C.-K. Lee, J. Ihm, and Y. Kuk, Phys. Rev. Lett. **90**, 216107 (2003).
[8] M. Ishigami, H. J. Choi, S. Aloni, S. G. Louie, M. L. Cohen, and A. Zettl, Phys. Rev. Lett. **93**, 196803 (2004).
[9] H. Kim, J. Lee, S. J. Lee, J.-Y. Park, S.-J. Kahng, and Y. Kuk, Phys. Rev. B **71**, 235402 (2005).
[10] L. Chico, V. H. Crespi, L. X. Benedict, S. G. Louie, and M. L. Cohen, Phys. Rev. Lett. **76**, 971 (1996).
[11] R. Saito, G. Dresselhaus, and M. S. Dresselhaus, Phys. Rev. B **53**, 2044 (1996); J. C. Charlier, T. W. Ebbesen, and Ph. Lambin, *ibid.* **53**, 11108 (1996).
[12] L. Chico, L. X. Benedict, S. G. Louie, and M. L. Cohen, Phys. Rev. B **54**, 2600 (1996).
[13] L. Chico, M. P. López Sancho, and M. C. Muñoz, Phys. Rev. Lett. **81**, 1278 (1998); C. G. Rocha, T. G. Dargam, and A. Latgé, Phys. Rev. B **65**, 165431 (2002); W. Zhang, W. Lu, and E. G. Wang, *ibid.* **72**, 075438 (2005); F. Triozon, P. Lambin, and S. Roche, Nanotechnology **16**, 230 (2005); E. Jódar, A. Pérez-Garrido, and A. Díaz-Sánchez, Phys. Rev. B **73**, 205403 (2006).
[14] L. Chico and W. Jaskólski, Phys. Rev. B **69**, 085406 (2004); W. Jaskólski and L. Chico, *ibid.* **71**, 155405 (2005).
[15] With one π orbital per atom, the hopping parameter for nearest neighbors is fixed to $V_{pp\pi}=-2.66$ eV.
[16] A. Ayuela, L. Chico, and W. Jaskólski, Phys. Rev. B **77**, 085435 (2008).
[17] J. P. Perdew, K. Burke, and M. Ernzerhof, Phys. Rev. Lett. **77**, 3865 (1996).
[18] J. M. Soler, E. Artacho, J. D. Gale, A. García, J. Junquera, P. Ordejón, and D. Sánchez-Portal, J. Phys.: Condens. Matter **14**, 2745 (2002).
[19] J. E. Ortega and F. J. Himpsel, Phys. Rev. Lett. **69**, 844 (1992); A. Ayuela, E. Ogando, and N. Zabala, Phys. Rev. B **75**, 153403 (2007).
[20] M. Fujita, K. Wakabayashi, K. Nakada, and K. Kusakabe, J. Phys. Soc. Jpn. **65**, 1920 (1996); K. Wakabayashi, M. Fujita, H. Ajiki, and M. Sigrist, Phys. Rev. B **59**, 8271 (1999).
[21] Y. Gan, L. Sun, and F. Banhart, Small **4**, 587 (2008).
[22] A. Ayuela, W. Jaskolski, M. Pelc, H. Santos, and L. Chico, Appl. Phys. Lett. **93**, 133106 (2008).